Geobios 49 (2016) 177–189

Available online at
ScienceDirect
www.sciencedirect.com

Elsevier Masson France
EM|consulte
www.em-consulte.com

Original article

Ontogeny and evolution within the Myophorellidae (Bivalvia): Paedomorphic trends☆

Javier Echevarría

CONICET – División Paleozoología de Invertebrados, Museo de La Plata, Paseo del Bosque s/n, 1900 La Plata, Buenos Aires Province, Argentina

ARTICLE INFO

Article history:
Received 16 June 2015
Accepted 20 January 2016
Available online 30 April 2016

Keywords:
Steinmanella
Myophorella
Promyophorella
Geometric morphometry
Deceleration
Heterochrony
Paedomorphocline

ABSTRACT

The role of heterochronic phenomena in molluscan evolution is insufficiently understood but potentially significant. The aim of this paper is to explore some paedomorphic trends in the evolution of the Myophorellidae (Bivalvia: Trigoniida). Early ontogeny of general shell shape and ornamentation of one species of *Steinmanella* was analyzed and compared to data obtained for three species of *Myophorella*: two belonging to the subgenus *M. (Promyophorella)* (one from the Jurassic and one from the Cretaceous) and one belonging to the Jurassic *M. (Myophorella)*. For general shell shape, a geometric morphometric analysis was performed on lateral views of the shells. Regarding ornamentation, flank costal disposition on the marginal carina, tubercle separation and relative development of the sub-commarginal subset of flank costae were quantified. A qualitative analysis was also performed. A two-trend shell shape development is considered as primitive. The first trend is marked by a relative reduction of the posterior margin together with a relative elongation of the shell. A tangential opisthogyrate growth component characterizes the second trend. There is a transitional stage where both trends interact. Early flank ornamentation is characterized by two or three sub-commarginal costae, continuous through the area, after which oblique costae with fine tubercles start to form. The subgenus *M. (Myophorella)* evolved by paedomorphic retention of juvenile shell shape and ornamentation, resulting in a large shell with coarse tubercles. Shell morphology in *Steinmanella* evolved by paedomorphic suppression of the primitive second trend in the development of the shell, resulting in an orthogyrate shell shape, and the retention of juvenile ornamentation (coarse tubercles, more sub-commarginal costae, juvenile rates of costal disposition). The paedomorphic (most likely by deceleration) retention of juvenile shell morphology within the Myophorellidae seems to have been recurrent within the group, resulting in many cases of convergence, and obscuring the phylogenetic relationships among its species.

1. Introduction

The importance of morphological variation through ontogeny among the Trigoniida was recognized long time ago, mostly to assess the evolutionary relationships between taxa (Hall, 1901; Kobayashi, 1954; Kobayashi and Amano, 1955; Kobayashi and Mori, 1955; Kobayashi and Tamura, 1955; Kelly, 1995; Lazo, 2003; Rudra and Bardhan, 2006). Nevertheless, few papers dealt with detailed descriptions of that ontogenetic variation (March, 1911; Maeda and Kawabe, 1966; Echevarría, 2014a) and references to heterochronic processes acting on the group are scarce (Francis and Hallam, 2003: p. 300; Rudra and Bardhan, 2006: p. 624; Cooper, 2015: p. 17, 19, 23–24).

The family Myophorellidae was proposed by Cooper (1991) to include species with generally conspicuously nodate and oblique flank ribs, although with sub-commarginal flank costae in early growth stages (Fig. 1). The genus *Myophorella* Bayle includes a wide range of species with these general characters. Kobayashi and Tamura (1955) ordered its variability subdividing the genus into three subgenera: *Myophorella* s.s., *Promyophorella* Kobayashi and Tamura, and *Haidaia* Crickmay. *Myophorella* s.s. was characterized by having a typical triangular shell with strong tubercles on the flank (Fig. 1(G)). *Promyophorella*, on the other hand, had a more varied shell outline (often crescentic), ornamented by narrower costae on the flank, with small tubercles aligned on the top (Fig. 1(E)). As suggested by its name, this subgenus was regarded as the ancestor of the other two by Kobayashi and Tamura (1955). The genera *Steinmanella* Crickmay and *Quadratotrigonia* Dietrich were considered by Kobayashi and Amano (1955) as two independent offshoots of the Myophorellinae. They share with *Myophorella* s.s.

☆ Corresponding editor: Emmanuel Fara.

E-mail address: javierechevarria@fcnym.unlp.edu.ar

http://dx.doi.org/10.1016/j.geobios.2016.01.015
0016-6995/

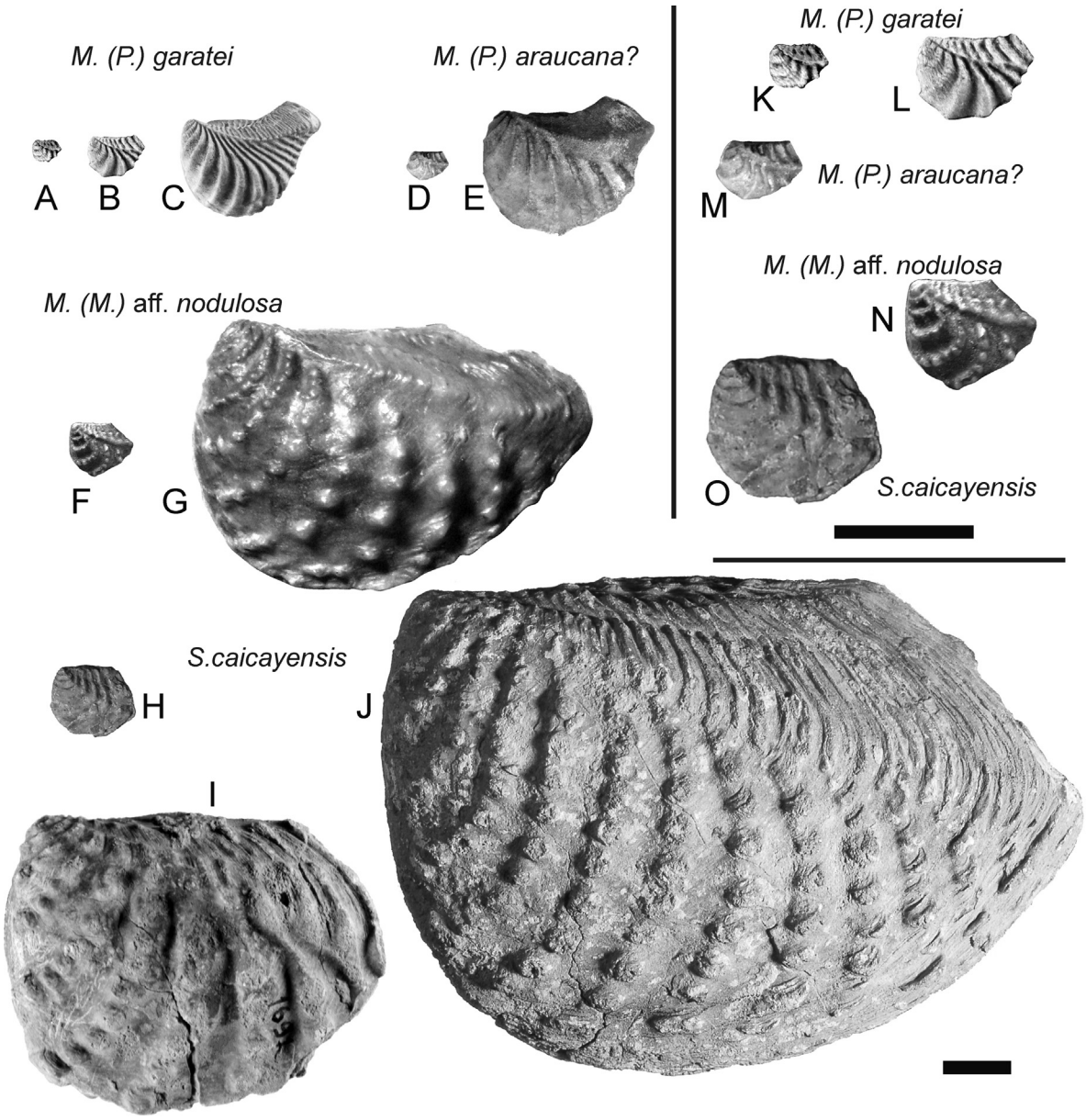

Fig. 1. Photographs of the species analysed in this study. **A–C**. *Myophorella garatei* H. Leanza, Museo Municipal Carmen Funes, Plaza Huincul, Argentina (MCF-PIPH)-428; A, B, juvenile stages recovered from growth lines in left lateral view; C, adult shell in left lateral view. **D, E**. *Myophorella araucana?* (A. Leanza), Servicio Nacional de Geología y Minería, Santiago, Chile (SNGM)-604; D, right valve juvenile stage recovered from a growth line (mirrored for comparison); E, adult shell of the individual D in left lateral view. **F, G**. *Myophorella* aff. *nodulosa* (Lamarck), Museo Provincial de Ciencias Naturales "Dr. Prof. Juan A. Olsacher", Zapala, Argentina (MOZ-Pi)-2330; F, left valve juvenile stage recovered from a growth line; G, adult shell of the individual F in right lateral view (mirrored for comparison). **H–J**. *Steinmanella caicayensis* Lazo and Luci; H, MCF-PIPH-410, juvenile shell in left lateral view; I, Museo de La Plata, La Plata, Argentina (MLP)-34627, middle-sized shell in left lateral view; J, MLP-34630/4, adult shell in right lateral view. **K–O**. Detail of the juveniles of all species; K, L, *M. garatei*, MCF-PIPH-428 (same shells as A, B); M, *M. araucana?*, SNGM-604 (same shell as D); N, *M.* aff. *nodulosa*, MOZ-Pi-2330 (same shell as F); O, *S. caicayensis*, MCF-PIPH-410 (same shell as H). Scale bars: 10 mm (A–J, K–O).

the presence of strong tubercles on flank costae, but they differ from it in having an area surface barely differentiated from the flank. While *Steinmanella* is more similar to *Myophorella* s.s. in shell outline (Fig. 1(J)), *Quadratotrigonia* is more quadrate, being truncated at both anterior and posterior ends.

This general evolutionary scheme was followed later on by many authors (Levy, 1966; Pérez and Reyes, 1977; Fleming, 1987; H. Leanza and Garate-Zubillaga, 1987; Cooper, 1991; H. Leanza, 1993; Francis and Hallam, 2003) although sometimes the taxa were grouped under different generic names and some species were variably referred to different genera. As a result, the Myophorellidae remains as one of the unresolved clades within Trigoniida (Schneider and Kelly, 2014).

Heterochrony focuses on the study of evolution as a consequence of regulation in timing and rates of development within a structurally conserved ontogeny (McKinney and McNamara, 1991). In this paper, the early ontogeny of general shell shape and ornamentation of four species, representing three of the main morphologies within the Myophorellidae, were analysed, together with their stratigraphic distribution. The main goal was to establish the generalized ontogeny for this family and to understand the heterochronic phenomena which may have been involved in the evolution of those morphologies. This will lead to a better understanding of the systematics of the group. The studied species are *Myophorella (Promyophorella) araucana?* (A. Leanza) from the Pliensbachian of Chile, *Myophorella (Myophorella)* aff.

nodulosa (Lamarck) from the Callovian of France, *Steinmanella caicayensis* Lazo and Luci, and *Myophorella (Promyophorella) garatei* H. Leanza, both from the Valanginian of Argentina.

2. Material and methods

2.1. Material

Data for the analysed material are summarized in Table 1. Although *M.* aff. *nodulosa* is represented by only two shells, their fine preservation allowed the identification of 15 landmark configurations at different ontogenetic stages. These shells are labelled as *Myophorella clavellata* (Parkinson), which according to Francis and Hallam (2003) is a junior synonym of *M. nodulosa* (Lamarck). Nevertheless, the stratigraphic range of *M. nodulosa* is from the Early Oxfordian to the Early Kimmeridgian (Francis and Hallam, 2003), so it is highly probable that the studied material belongs to a Callovian taxon related to *M. nodulosa*, like *M. irregularis* (Seebach). Here, they will be referred to as *M.* aff. *nodulosa*.

The sample from a single locality in Chile was referred to *Myophorella araucana* (A. Leanza) by Pérez et al. (2008). Nevertheless, the type material of the species described by A. Leanza (1942) – MLP 3904, 6253, 6708, 6724, 6735 – from the Late Pliensbachian of Neuquén, Argentina, is actually a bit different in shell shape. Since a systematic revision of the species is beyond the scope of this paper, the studied material will be here referred to as *M. araucana?*

The Cretaceous species *Myophorella garatei* was used for comparison only for the general shell shape analysis since its ontogeny is well known (Echevarría, 2014a).

2.2. Methods

One central aspect of heterochronic analyses is the comparison of ontogenies among related lineages. Having an evolutionary sequence, knowledge of ontogenetic age is a requirement in order to fully understand the underlying heterochronic changes. Nevertheless, ontogenetic data, even without chronological age associated, provide useful information. As a consequence, study of allometry has been considered an integral part of heterochronic analysis (McKinney, 1988). Biological age information is unavailable for the studied specimens. Although the relationship between size and shape alone is good enough to establish the ontogenetic changes within a species, it is inadequate to determine heterochronic processes. So, the conclusions attained in this paper about the processes producing the observed patterns must be considered as allometric heterochrony (McKinney, 1988; Crampton and Maxwell, 2000), although the potential implications of the heterochronic processes implied will be also discussed.

Shape was quantified for different ontogenetic stages within the different species. This could not be achieved for some characters and thus, a qualitative description was also undertaken. All measured parameters were compared to size in order to establish the allometric trends in the development of each species. The development of *M. araucana?* was considered as the primitive reference, since it is one of the earliest members of the genus, and the development of the other species was compared to it to check for similarities and differences. Two main characters were measured, general shell shape and ornamentation, each one requiring specific methods.

2.2.1. General shell shape analysis

Procrustres-superimposed configurations of landmarks and semi-landmarks are the basic shell shape data quantified for this analysis. A geometric morphometric analysis of the shells (including juvenile stages based on growth lines) was performed following the procedures outlined by Zelditch et al. (2004). This was done on lateral view photographs and camera lucida drawings. The landmark and semi-landmark configurations (Fig. 2(B)) were established as in Echevarría (2014a). Finally, a PCA was performed to visualize the main shape variations between configurations.

Size was quantified as the natural logarithm of centroid size, or ln(CS) for these data. Multivariate linear regressions for the different post-larval stages identified were performed to establish the relationship between size and shape. The significance of the dependence of shape on size was evaluated by means of the Procrustes F-Test, a resampling-based version of Goodall's F-test based on 1000 bootstrap replicates (Zelditch et al., 2004: p. 224–225).

Geometrically speaking, the regression equation of shape variables on size (the independent variable) is a vector. The angle between two regression vectors provides a comparison between them, the cosine of that angle (r_v) being their correlation (Zelditch et al., 2004: p. 251): low angles imply high correlations, while orthogonal vectors result in no correlation ($r_v = 0$), implying that the two regressions are independent. The bootstrap procedure established by Zelditch et al. (2004: p. 251–252) was applied to test for significance of the angle between regressions, i.e., significance of the difference between two ontogenetic trajectories.

Digitization of the landmark configurations was performed using TPSdig 2.12 (Rohlf, 2008). Procrustes superimposition was done with CoordGen 6h (Sheets, 2001); semi-landmark sliding (to perpendicular alignment on the reference) was developed on SemiLand 6 (Sheets, 2003); PCAGen 6p (Sheets, 2001) was used to perform principal component analysis (PCA). Regress 6N and VecCompar 6c (Sheets, 2003) were used for regression analyses.

2.2.2. Ontogenetic morphospace

Considering the importance of *M. garatei* data as a reference for the shell shape ontogenetic analysis, a particular morphospace for this dataset was first constructed. The aim of this analysis was to order the data in such a way that the first ordination axis would encompass the allometric shape variation expressed on the first stage of development of that species. The second axis, ideally, would contain the main allometric shape

Table 1
Collection data of the analyzed material.

Sample	Species	Number of shells	Number of landmark configurations	Age	Provenance
SNGM 596, 597, 600, 602, 604, 606, 609 and 613	*M. araucana?*	8	16	Pliensbachian	Qda. Asientos, Atacama, Chile
MOZ-Pi-2324 and 2330	*M.* aff. *nodulosa*	2	15	Callovian	Villiers, Calvados, France
MLP-34627 to 34633	*S. caicayensis*	24	42	Valanginian	Co. La Parva, Neuquén, Argentina
MCF-PIPH 410	*S. caicayensis*	9	28	Valanginian	Ao. Rahueco, Neuquén, Argentina
MCF-PIPH 427 to 429	*M. garatei*	45	86	Late Valanginian	Co. Mesa, Neuquén, Argentina

M. araucana: *Myophorella araucana*; *M.* aff. *nodulosa*: *Myophorella* aff. *nodulosa*; *S. caicayensis*: *Steinmanella caicayensis*; *M. garatei*: *Myophorella garatei*; SNGM: Servicio Nacional de Geología y Minería, Santiago, Chile; MOZ-Pi: Museo Provincial de Ciencias Naturales "Dr. Prof. Juan A. Olsacher", Zapala, Argentina; MCF-PIPH: Museo Municipal Carmen Funes, Plaza Huincul, Argentina; MLP: Museo de La Plata, La Plata, Argentina.

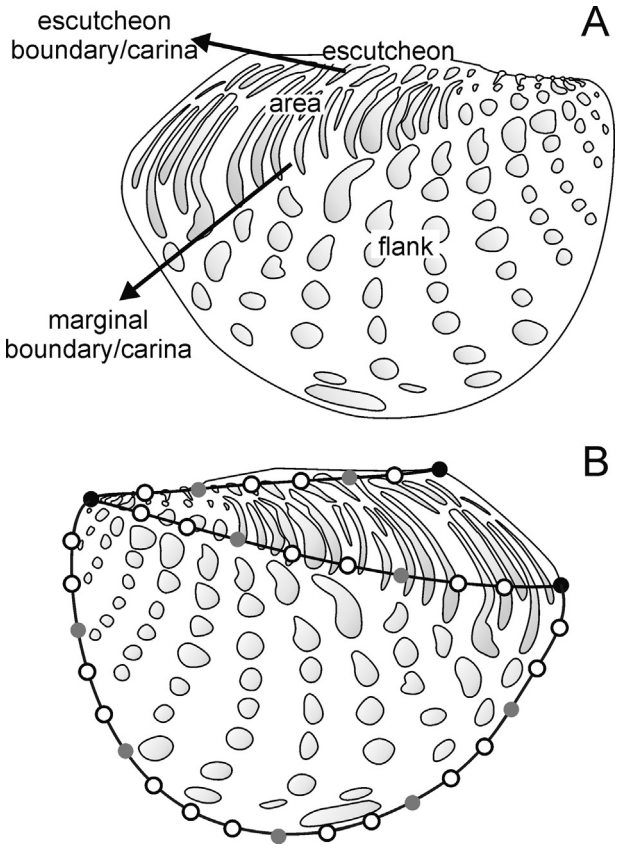

Fig. 2. A. Schematic drawing of a trigoniid shell showing the main morphological features. **B**. Landmarks and semi-landmarks used in the geometric morphometric analysis; black dots, landmarks; grey dots, semi-landmarks; white dots, helper points.

variation contained on the second stage of development. For comparative purposes, the data of the remaining species was projected in that morphospace.

The first axis of this ontogenetic morphospace (from now on OM1) was obtained through a PCA of the landmark configurations representing the first ontogenetic stage alone (CS lower than 10; see Section 3.2). PC1 of this PCA was used as OM1. Then, the remaining data of *M. garatei* (landmark configurations for the transitional and second ontogenetic stages) were projected on the obtained principal components (PCs) for the first stage. To do so, the scores on the PCs for each individual were calculated by multiplying the original data (i.e., the position values of the landmarks after Procrustres superimposition) by the corresponding eigenvectors. Using the scores of each individual for PCs 2 to 24, a new PCA was performed for the whole ontogenetic data set. These new PCs were used as the remaining axes of the ontogenetic morphospace (from now on OM2-24). In this way, the ontogenetic variation of the first stage was encompassed by OM1 alone, while the remaining ontogenetic variation was encompassed by the remaining OMs. To check if the obtained axes truly express the allometric variations expected, correlations with ln(CS) were calculated for the first 11 OMs (encompassing 95% or more of the variance for each stage). The PCAs and correlation calculations were performed on the software PAST 2.17 (Hammer et al., 2001) while the projection of new data on those PCs was performed on a standard spreadsheet software.

2.2.3. Ornamentation analysis

The quantified ornamentation characters include: flank costal disposition on the marginal carina, tubercle separation and relative extent of the sub-commarginal subset of flank costae. Nevertheless, since ornamentation among trigoniids can be highly variable, these measurements were supplemented by a general qualitative analysis. Fig. 2(A) shows the descriptive terminology for trigoniid shells.

Flank costal disposition on the marginal carina was quantified following the procedures established by Echevarría (2013). An ordinary least squares regression was obtained from the log-transformed values of distance from each costa to the umbo (x) and the log-transformed values of distance from each costa to the next costa (y). The coefficients obtained were considered as descriptors of costal disposition. The slope describes its pattern: higher values imply a progressive separation of costae as size increases, lower values imply a more even arrangement of costae. The intercept is an approximation of the basic intercostal distance, higher values implying a looser disposition. In order to check for changes in relative rates of costal production, this analysis was also applied to size-standardized data. To do so, distance values from each costa to the umbo and from each costa to the next costa were all divided by the largest distance to the umbo within each species. In this way, all data were scaled according to the adult size of the species. This transformation may cause a change in the intercept value (i.e., the intercept value also contains scaling information), but not in the slope value.

To check for retention of juvenile rates of costal production on the carina from the primitive (*M. araucana?*) ornamentation, the following exercise was proposed: from two preestablished parameters the values of costal disposition along the carina were calculated. From these data, a new dataset was generated by duplication of the costae, always maintaining their values of disposition (i.e., if costal separation in the first set was 0.136, 0.170, 0.208. . ., the sequence for the second set would be 0.136, 0.136, 0.170, 0.170, 0.208, 0.208. . .). In this way, the rate of juvenile costal production was retained longer. New values of slope and intercept were calculated for this second data set.

Tubercle separation was also measured, considering different growth stages. For this character, shell height was used as size estimator. Separation values were measured from the costa closest to the most ventral point of the shell. When only few data were available (especially on smaller shells), the anterior and posterior costae were also considered. In order to have a single value for each height datum, the mean value was obtained in each case. It was also treated as relative separation (i.e., separation/height) and it was compared to the height and to standardized height (i.e., height/maximum height for the species). For each species an allometry coefficient (a.c.) was calculated together with the probability of a.c. being one (i.e., the relationship between variables being isometric). Measurements were performed from lateral view photographs using the software ImageJ 1.37, while comparisons and allometry analyses were performed using PAST 2.17 (Hammer et al., 2001).

The relative development of the sub-commarginal subset of flank costae was measured and compared to the marginal carina length in adult shells. These data were measured on dorsal view photographs (Fig. 3) using ImageJ 1.37.

3. Results

3.1. General PCA

Results for the PCA of shell shape in lateral view are shown on Fig. 4. Size within each sample is negatively correlated to PC1 (i.e., ontogeny in the graph goes from right to left). *S. caicayensis* and most of *M.* aff. *nodulosa* samples overlap with the first ontogenetic stage of *M. garatei*.

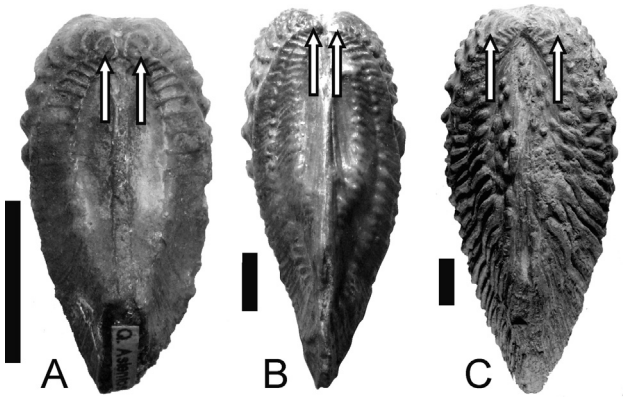

Fig. 3. Dorsal views of the analysed species. **A**. *Myophorella araucana?*, Servicio Nacional de Geología y Minería, Santiago, Chile (SNGM)-604. **B**. *Myophorella* aff. *nodulosa*, Museo Provincial de Ciencias Naturales "Dr. Prof. Juan A. Olsacher", Zapala, Argentina (MOZ-Pi)-2330. **C**. *Steinmanella caicayensis*, Museo de La Plata, La Plata, Argentina (MLP)-34628. Arrows show the last sub-commarginal rib of the flank at the carinae. Scales bars: 10 mm.

3.2. M. garatei *and the ontogenetic morphospace*

The ontogenetic morphospace constructed for *M. garatei* is shown on Fig. 5. As expected, size for the first growth stage configurations is significantly correlated only to OM1, while size at the second growth stage shows the strongest correlation with OM2, although it also has a significant correlation with other ordination axes (Table 2). During the development of *M. garatei*, a transitional stage could be differentiated from the first stage previously established (Echevarría, 2014a). This transitional stage develops between CS of 10 and 20 (i.e., between 4 mm and 8 mm umbo-posterior point distance). Size at this stage is strongly correlated with OM1 and OM2 (Table 2), indicating its transitional character.

When the ontogenetic vectors of the different stages within *M. garatei* are compared (Table 3), the first stage is indistinguishable from the transitional stage, while both of them are significantly different from the second stage. Size during the second ontogenetic stage bears no correlation with OM1 (Table 2), and its regression is almost orthogonal to that of the first stage (Table 3), implying that the first trend of change has already stopped during the second stage.

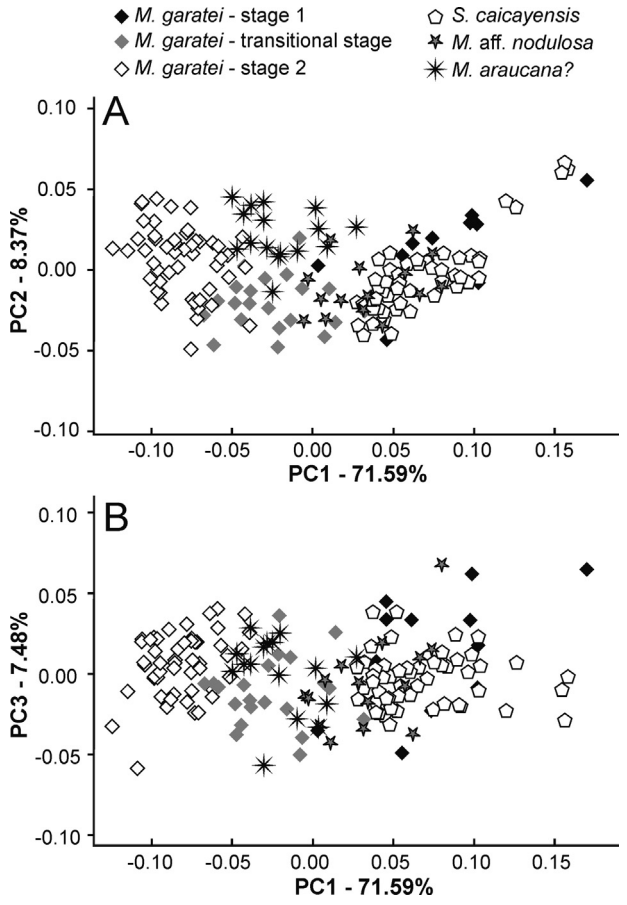

Fig. 4. PCA of the Procrustes coordinates of landmark and semi-landmark configurations. **A**. First *vs*. second principal components, accounting for 71.59% and 8.37% of the total variance, respectively. **B**. First *vs*. third principal components, accounting for 71.59% and 7.48% of the total variance, respectively.

3.3. Shell shape in the studied species

A significant correlation between size and shell shape was found for *M. araucana?* (bootstrapped $P = 0.002$; 23.8% of variance explained), *M.* aff. *nodulosa* (bootstrapped $P = 0.019$; 19.2% of variance explained), and *S. caicayensis* (bootstrapped $P < 0.001$; 42.5% of variance explained). Fig. 6 shows the main ontogenetic changes for each species.

The data for *M. araucana?* seem to correlate better to the second growth stage of *M. garatei* than to the first one (Table 3; Fig. 5(B)), although the strongest correlation is with the transitional stage (Table 3). The data for *M.* aff. *nodulosa* and *S. caicayensis* are strongly related to OM1 (Fig. 5(C, D)). In both cases there seems to be a linear trend instead of a two-stages development. When growth vectors are compared (Table 3), the second growth stage of *M. garatei* is uncorrelated with, and almost orthogonal to both of them. In *M.* aff. *nodulosa*, the shell shape reaches the morphologies typical of the transitional stage, while in *S. caicayensis* shell morphology is well within the morphospace of the first stage (Fig. 4). Ontogeny in both taxa is indistinguishable (Table 3), although in *M.* aff. *nodulosa* the escutcheon carina seems to curve dorsally at the posterior end (Fig. 6(E)).

Size, considered as ln(CS), strongly correlates to OM1 in *Steinmanella* (Fig. 5(D)), although it also shows some correlation with other axes (including OM2 and OM3). The analysed sample is very close to the first ontogenetic stage in the morphospace. The main difference seems to be in the smaller configurations, which in *Steinmanella* are a little bit longer and have a more curved marginal carina. As size increases, both morphologies tend to converge. The comparison of its growth vector with the first stage of *M. garatei* shows no significant difference and a high correlation (Table 3).

3.4. Description of the ornamentation

Escutcheon ornamentation is different among species. Some shells of *M. araucana?* bear a smooth escutcheon (Fig. 3(A)), while most of them show transverse ribs variably developed, crossing from the area. In *M.* aff. *nodulosa* no ornamentation could be found in the escutcheon (Fig. 3(B)), while in *S. caicayensis*, commarginally aligned tubercles (sometimes loosely aligned in transverse rows) could be found (Fig. 3(C)).

Area ornamentation is very conservative within the group, usually showing continuous transverse costae on the anterior portion, separating progressively and fading in later stages. This general pattern was already recognized by Crickmay (1932). *M. araucana?* and *M.* aff. *nodulosa* tend to bear a smooth area posteriorly, only crossed by conspicuous growth lines (Figs. 1(E, G), 3(A, B)). *S. caicayensis* bears an almost smooth middle portion of the area, while posteriorly it develops strong commarginal rugae (Fig. 3(C)). Usually, in later stages these rugae can invade the flank

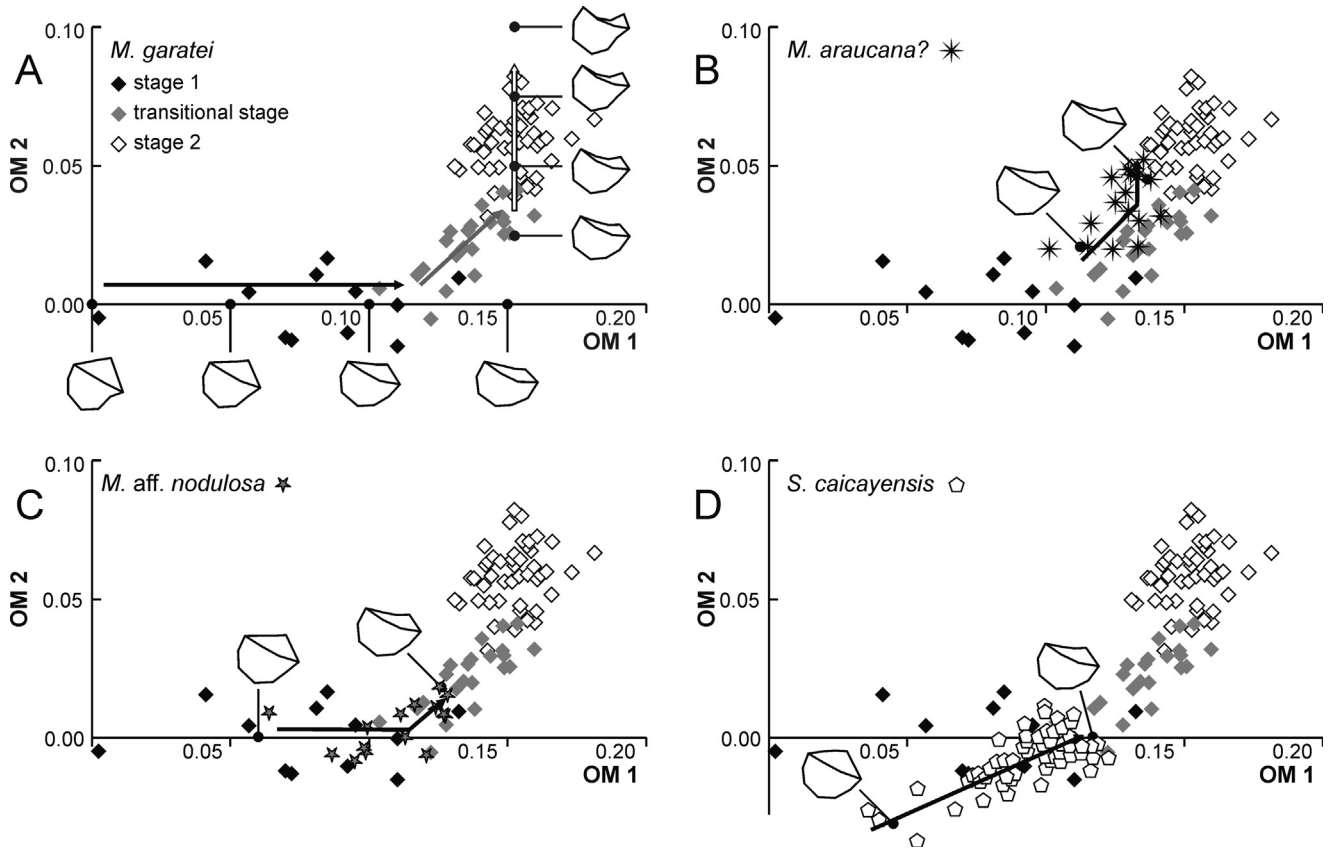

Fig. 5. Ontogenetic morphospace based on the data of *Myophorella garatei*. **A**. OM1 *vs*. OM2, showing the main morphologic changes associated with each axis. **B**. Data for *Myophorella araucana?* projected onto the OM1–OM2 morphoplane. **C**. Data for *Myophorella* aff. *nodulosa* projected onto the OM1–OM2 morphoplane. **D**. Data for *Steinmanella caicayensis* projected onto the OM1–OM2 morphoplane. Arrows show the main directions of size increase.

(Fig. 1(J)). The submedian sulcus in the area is barely developed in *M. araucana?*, but it is clearly present on the other species. In *M.* aff. *nodulosa* and *S. caicayensis* a row of tubercles is associated with it, although in the latter they disappear when the rugae are developed. Carinae are usually developed among *Myophorella* species, especially in early ontogenetic stages. In *M. araucana?* they develop later on as rounded angulations between the area and the other surfaces of the shell (the escutcheon and the flank; Figs. 1(E), 3(A)). In *M.* aff. *nodulosa* these angulations are broader and less defined (Figs. 1(G), 3(B)). *S. caicayensis* only shows a sharp angulation between the area and the other surfaces on the initial stages (Figs. 1(H, O) and 3(C)). Later on, the area surface is almost continuous with those of the escutcheon and the flank, being differentiated mostly by ornamentation (Fig. 1(I, J)). Area boundaries of the three studied species usually bear tubercles, coinciding with the costae anteriorly and free posteriorly. In *Steinmanella* tubercles develop posteriorly as a widening of the rugae.

Flank costal development is very similar among species of the group. The first costae (2 or 3 in *Myophorella* species, up to 5 in *Steinmanella*) are sub-commarginal and continuous with those on the area, usually smooth, in a pattern that resembles the genus

Table 2
Variance explained by each of the main axes of the ontogenetic morphospace and correlation to size data along those OMs for *M. garatei* within each stage of development of this species.

	Stage 1				Transition stage				Stage 2			
Axis	$r_{ln(CS)}$	p_r	%var	Cumulative	$r_{ln(CS)}$	p_r	%var	Cumulative	$r_{ln(CS)}$	p_r	%var	Cumulative
OM1	−0.956	$1.22 \times 10^{-6***}$	0.612	0.612	−0.702	$2.68 \times 10^{-4***}$	0.221	0.221	0.06	0.673	0.133	0.133
OM2	−0.087	0.788	0.0664	0.679	−0.742	$7.6 \times 10^{-5***}$	0.171	0.392	−0.762	$5.5 \times 10^{-11***}$	0.173	0.306
OM3	−0.056	0.862	0.121	0.800	−0.112	0.620	0.249	0.641	0.0499	0.725	0.249	0.555
OM4	0.118	0.716	0.0448	0.845	0.445	0.0379*	0.0632	0.704	−0.454	$7.25 \times 10^{-4***}$	0.171	0.725
OM5	−0.096	0.766	0.0375	0.882	−0.0153	0.946	0.0969	0.801	0.193	0.170	0.0495	0.775
OM6	0.171	0.596	0.0259	0.908	0.0273	0.904	0.0645	0.866	0.269	0.0537	0.0599	0.835
OM7	0.084	0.795	0.0313	0.940	−0.241	0.281	0.0252	0.891	0.409	$2.64 \times 10^{-3**}$	0.0379	0.873
OM8	−0.074	0.820	0.0144	0.954	0.0732	0.746	0.0146	0.906	−0.150	0.288	0.0362	0.909
OM9	−0.177	0.582	0.0131	0.967	−0.447	0.0369*	0.0303	0.936	0.173	0.219	0.0198	0.929
OM10	−0.166	0.607	0.00462	0.972	0.132	0.558	0.0160	0.952	−0.0366	0.797	0.0196	0.948
OM11	0.095	0.770	0.00442	0.976	−0.298	0.177	0.0127	0.965	−0.196	0.164	0.0107	0.959

OM: ontogenetic morphospace axes; *M. garatei*: *Myophorella garatei*. Size expressed as ln(CS).
* $0.01 < P < 0.05$.
** $0.001 < P < 0.01$.
*** $P < 0.001$.

Table 3
Comparison between ontogenetic vectors.

Vector #1	Vector #2	Angle between V1 and V2	r_v
Stage 1	Transition stage	44.7°	0.71
Transition stage	Stage 2	69.7°	0.35*
Stage 1	Stage 2	93.2°	−0.06*
M. araucana?	Stage 1	64.4°	0.43*
M. araucana?	Transition stage	47.5°	0.68
M. araucana?	Stage 2	55.6°	0.56*
Steinmanella	Stage 1	32.0°	0.85
Steinmanella	Transition stage	31.7°	0.85
Steinmanella	Stage 2	89.2°	0.01*
M. aff. *nodulosa*	Stage 1	30.9°	0.86
M. aff. *nodulosa*	Transition stage	38.5°	0.78
M. aff. *nodulosa*	Stage 2	85.4°	0.08*
Steinmanella	*M.* aff. *nodulosa*	32.1°	0.85
Steinmanella	*M. araucana?*	61.9°	0.47*
M. aff. *nodulosa*	*M. araucana?*	61.4°	0.48

M. araucana: *Myophorella araucana*; *M.* aff. *nodulosa*: *Myophorella* aff. *nodulosa*.
* Indicates significant differences ($P < 0.05$) following the procedure established by Zelditch et al. (2004, pp. 251–252).

Table 4
Relative extent of the different flank costae type along the marginal carina.

	Length of the carina in contact with concentric ribs	Total length of the carina	Ratio
M. araucana?	0.091	2.470	0.037
	0.097	2.198	0.044
	0.101	3.000	0.034
	0.137	2.146	0.064
M. aff. *nodulosa*	0.103	4.651	0.022
	0.126	6.876	0.018
Adult *S. caicayensis*	0.501	9.064	0.055
	0.744	9.126	0.082
	0.404	8.866	0.046
Juvenile *S. caicayensis*	0.701	(9.126)	0.077
	0.467	(9.126)	0.051
	0.663	(9.126)	0.073
	0.643	(9.126)	0.070
	0.421	(9.126)	0.046
	0.526	(9.126)	0.058

M. araucana: *Myophorella araucana*; *M.* aff. *nodulosa*: *Myophorella* aff. *nodulosa*; *S. caicayensis*: *Steinmanella caicayensis*. Ratios for juveniles of *S. caicayensis* were calculated using the largest carina length within adult shells (value within parenthesis).

Frenguelliella A. Leanza. The next group of costae (3 or 4 in *Myophorella* species, up to 6 in *Steinmanella*) develops a short portion perpendicular to the carina, followed by a posteriorly directed and anteriorly curved segment. This last segment is at a steep angle to the previous one. Usually at this stage tubercles start to appear. The remaining costae are interrupted by the development of the antecarinal smooth sulcus in both Jurassic species, causing the loss of the first segment (Fig. 1(E, G)). In *Steinmanella*, though developed, the sulcus does not interrupt the costae (Fig. 1(I, J)). In *M. araucana?* ribs are well defined, with tubercles developed on top of them. In *M.* aff. *nodulosa* and *S. caicayensis* tubercles are strong, knob-like and spaced, while costae are very low, mostly defined by the alignment of the tubercles.

3.5. Quantified ornamentation characters

Table 4 shows the absolute extent of sub-commarginal ribs on the flank, compared to the whole carina in adult shells. Relative separation between tubercles tends to decrease with size in *M. araucana?* (a.c. = 0.544, $p_{(a.c. = 1)} = 0.0015$) and *S. caicayensis* (a.c. = 0.605, $p_{(a.c. = 1)} = 0.0002$), while *M.* aff. *nodulosa* seems to show an isometric development of tubercles (a.c. = 0.966, $p_{(a.c. = 1)} = 0.8534$), although few data could be measured in this case. Both *S. caicayensis* and *M.* aff. *nodulosa* show high values of relative tubercle separation, even higher than juveniles of *M. araucana?* (Fig. 7(A)). When standardized height is considered (Fig. 7(B)) it seems that the data of the former two represent an earlier stage not measured or not expressed in *M. araucana?*

Regarding flank costal disposition on the carina (or the antecarinal sulcus in *M. araucana?*), *S. caicayensis* shows lower slope values than *M. araucana?* (Fig. 8(A)). Intercept values are slightly higher in *Steinmanella*, but when data are standardized, intercept values are clearly lower than in *M. araucana?* (Fig. 8(B)). No data are available for *M.* aff. *nodulosa*.

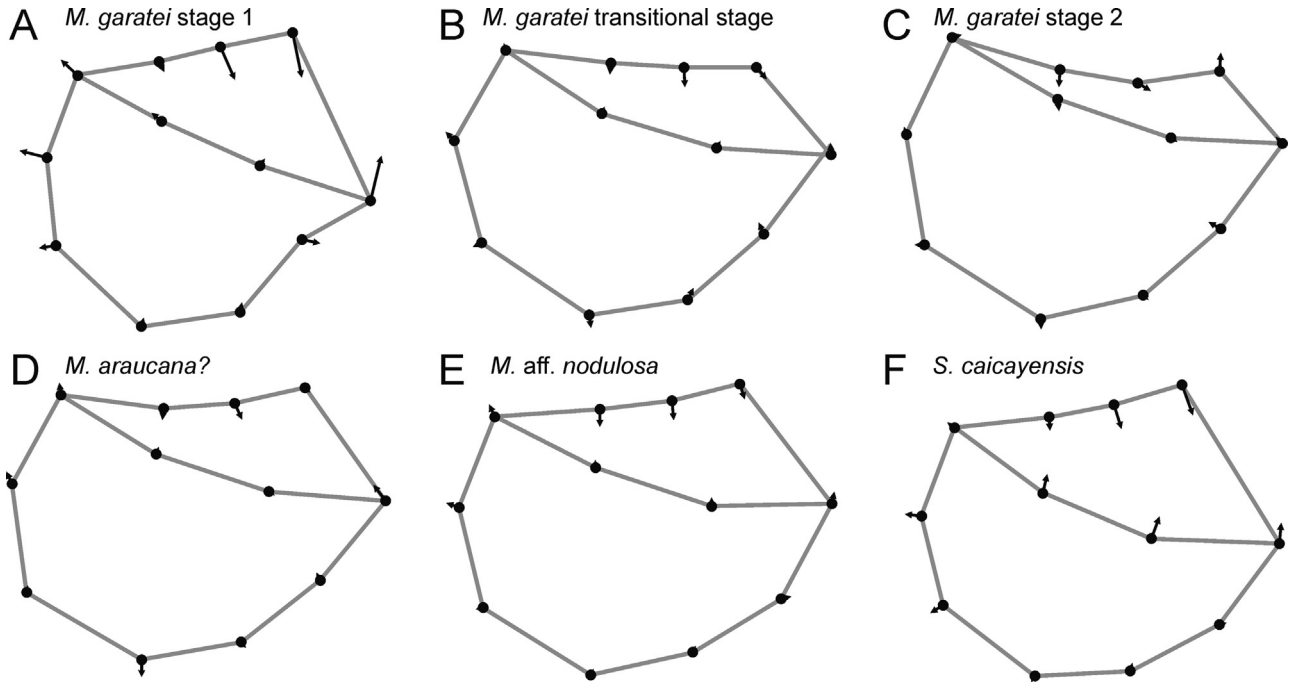

Fig. 6. Changes in landmark and semi-landmark positions with respect to size. **A–C**. Changes for *Myophorella garatei*; A, stage 1; B, transitional stage; C, stage 2. **D**. Changes for *Myophorella araucana?* **E**. Changes for *Myophorella* aff. *nodulosa*. **F**. Changes for *Steinmanella caicayensis*.

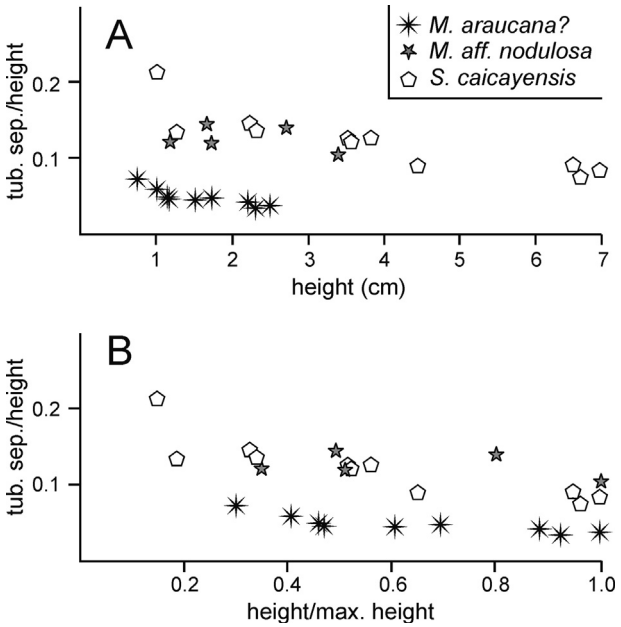

Fig. 7. Relative tubercle separation at different sizes. **A**. Data at their original scale; the tubercle separation/height ratio (y-axis) accounts for the mean tubercle relative separation. **B**. Size-standardized data.

A reduction of values for both indices was found after the retention of juvenile rates of costae disposition: from slope values of 0.734 and intercept of −0.567, the values of 0.530 for the slope and −0.692 for the intercept were obtained. This indicates that the paedomorph pattern should have more homogeneously and densely disposed costae.

4. Discussion

4.1. Shell shape in M. araucana*? and the primitive ontogenetic trajectory in* Myophorella

Since the ontogeny of shell shape in *M. garatei* is known in high detail, it was used as a basis for the comparison of other species within the group (Fig. 5). The general developmental pattern of this species can be summarized in three growth stages, as a result of two growth trends. The first trend of development is responsible for shell elongation and area reduction (Echevarría, 2014a), and is represented by OM1 (Fig. 5(A)). The second growth trend, represented by OM2 (Fig. 5(A)), is dominated by opisthogyrate growth and the development of the rostrum (Echevarría, 2014a). When compared to size, the first trend (OM1 scores) shows a clear asymptote (Fig. 9) beginning at ln(CS) of ∼3 (i.e., ∼8 mm umbo-posterior point distance) indicating the cessation point of this initial growth trend ("offset" *sensu* Reilly et al., 1997). Conversely, the change of scores for OM2, when compared to size, does not begin until a ln(CS) of 2.3 (i.e., ∼4 mm umbo-posterior point distance), indicating the onset of the second trend at this size (Reilly et al., 1997). This results in a first growth stage (with only the first growth trend developed), a transitional stage (with both growth trends developed) and a second stage (with only the second growth trend developed). The transitional stage would develop between the onset of the second growth trend (∼4 mm) and the cessation of the first one (∼8 mm).

Despite the detailed knowledge of the development of *M. garatei*, it cannot be considered as the primitive one within the group. *M. araucana?*, on the other hand, is one of the earliest records of the genus, and so its development can be considered as a proxy for the generalized developmental pattern of the lineage.

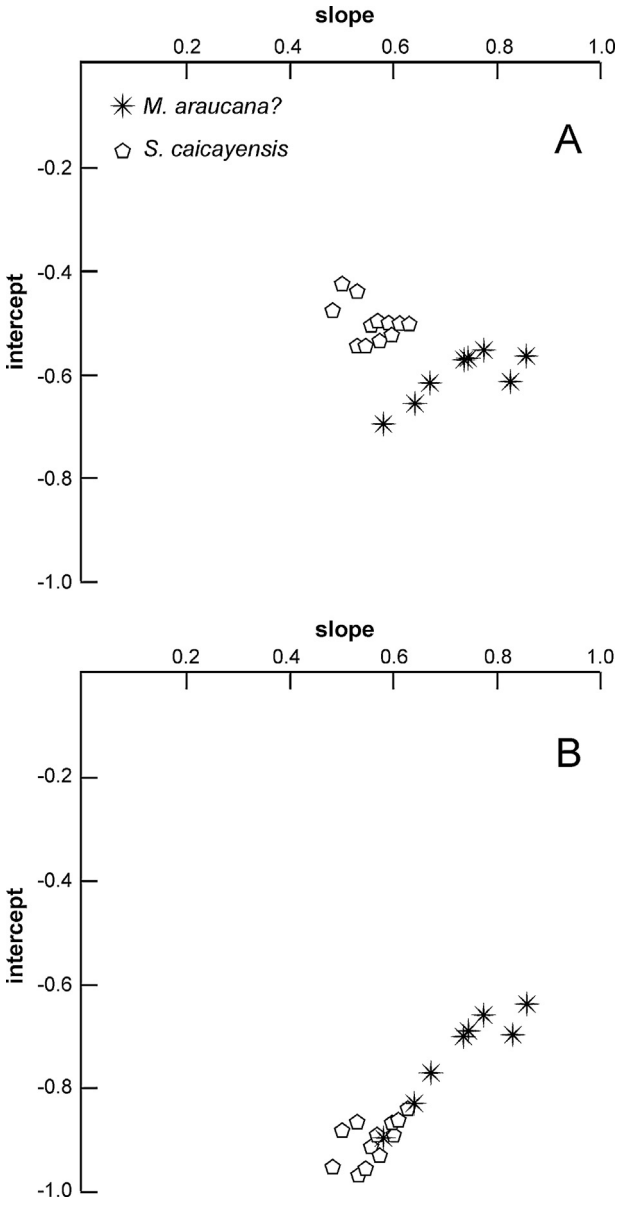

Fig. 8. Values of slope (*x*-axis) and intercept (*y*-axis) for costal disposition along the marginal carina. **A**. Data obtained from the values at their original scale. **B**. Data obtained from the size-standardized values.

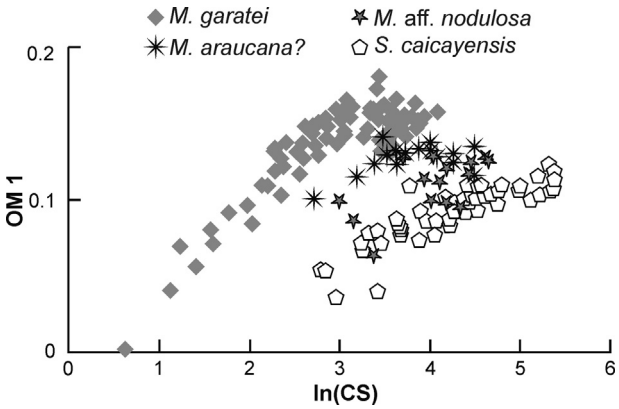

Fig. 9. Size [*x*-axis; in this case ln(CS)] *vs.* shape values (*y*-axis; in this case OM1 scores).

The ontogenetic trajectory for *M. araucana?* shows the greatest similarity with the transitional stage of *M. garatei* (Table 3; Fig. 6(B, D)). The main changes associated with size (Fig. 6(D)) are a dorsal curving of the area (indicating the action of an opisthogyrate component of growth), a slight antero-ventral expansion and a slight accentuation of the rostrum (most of the changes of the second growth trend), together with a reduction of the posterior margin (a change linked to the first growth trend). Nevertheless, when size data are compared with the scores for OM1, there is an asymptote (Fig. 9) indicating the cessation of the first ontogenetic trend at a ln(CS) of 3.7 (~ 15 mm umbo-posterior point distance); this can be seen as a short final trend parallel to OM2 (Fig. 5(B)). Interestingly, this cessation occurs at lower values of OM1 (Fig. 9), resulting in adults with a wider area than in *M. garatei*.

The onset of the second ontogenetic trend cannot be determined due to the scarcity of small configurations. Nevertheless, the middle-sized landmark configurations of the first growth stage of *M. garatei* are very similar to the smallest identified configurations for *M. araucana?* From this similarity a first developmental stage, similar to that found in *M. garatei*, can be assumed in the primitive ontogenetic trajectory. The myophorelloid *Scabrotrigonia eufaulensis* (Gabb) shows also a development comparable to the one of *M. garatei* (Echevarría, 2014b), suggesting the presence of this first stage (characterized only by the first growth trend) in the generalized developmental pattern for *Myophorella* and its descendants.

So the primitive growth pattern for the genus *Myophorella* has the same two growth trends found in *M. garatei*. Neither of them is developed as much as in the Cretaceous species, suggesting a peramorphic pattern for the latter, which disagrees with the statement about this species hinted by Cooper (2015: p. 19). At least the transitional and second growth stages were identified in *M. araucana?* and most likely the first growth stage is also developed. Nevertheless, some caution must be taken: despite the analysed sample of *M. araucana?* is one of the oldest for Myophorellidae, it is not the only one. Other *Myophorella* specimens from the Pliensbachian, with slightly different shell morphologies (A. Leanza, 1942; Pérez et al., 2008), were recorded, probably indicating somewhat different developmental patterns, although clearly opisthogyrate.

4.2. Paedomorphosis and the origin of the Myophorella s.s. condition

Although Pérez and Reyes (1977) and H. Leanza and Garate-Zubillaga (1987) considered *M. araucana* as belonging to the subgenus *Myophorella* s.s., the assignment to the subgenus *Promyophorella*, as suggested by Levy (1966), is more in line with the original proposal by Kobayashi and Tamura (1955). According to them, this subgenus was the ancestor of *Myophorella* s.s. They recognized that the typical forms of both subgenera are so different that two distinct genera could be represented, but the presence of many transitional forms between them precluded such treatment.

Kobayashi and Tamura (1955) also considered that *Myophorella* s.s. could be a polyphyletic taxon. The Late Jurassic (Kimmeridgian to Tithonian according to Sato and Taketani, 2008) species from Japan, *Myophorella (M.) dekaiboda* Kobayashi and Tamura, was differentiated from European species. The shell of the Japanese species has a somewhat quadrate shell outline and internally impressed ventral costae. Given these morphological features, together with its isolated geographic occurrence, a different origin from the European lineage was proposed for it. European *Myophorella* species were analyzed by Francis and Hallam (2003), who provided a summary of their evolution. According to them, *M. (P.) spinulosa* (Young and Bird) is the oldest species recorded there (Toarcian-Bajocian). It has an opisthogyrate shell, produced posteriorly and this (or other *Promyophorella*-like species) was ancestral to *Myophorella (M.) signata* (Agassiz). According to Francis and Hallam (2003) the derivation of one from another occurred by heterochronic change in the spacing and size of the tubercles, but also *M. (M.) signata* has a much-less opisthogyrate shell.

According to the data presented here, many of the characters of *Myophorella* s.s. can be considered as juvenile. Shell shape in *Myophorella* aff. *nodulosa* shows a very similar development to the first and transitional growth stages of *M. garatei* (and probably of the "primitive *Myophorella*"). The largest landmark configurations in *M.* aff. *nodulosa* strongly resemble "transitional morphologies" (Figs. 4 and 6(B, E)). The stout tubercles typical of the subgenus are strongly suggestive of the tubercles of a young *Promyophorella*-like shell enlarged due to the differences in shell size (Fig. 7(B)). Relative tubercle separation decreased with size in *M. araucana?*, suggesting that the large separation between tubercles found in *M.* aff. *nodulosa* (and probably also the large size of the tubercles themselves) is a retention of a juvenile character.

All these data strongly point toward a paedomorphic origin for the *Myophorella* s.s. shell morphology. Given the gradation between both taxa recognized by Kobayashi and Tamura (1955) and the possible polyphyly in *Myophorella* s.s., most likely *Promyophorella* and *Myophorella* s.s. represent grades within the genus instead of monophyletic taxa, with *Myophorella* arising more than once from *Promyophorella* by some heterochronic process. The sub-quadrate shell shape of *M. (M.) dekaiboda* and *M. (M.) signata* is then the retention of a juvenile morphology, while the spacing of tubercles is probably the result of a heterochronic process (Fig. 10), as suggested by Francis and Hallam (2003).

4.3. Paedomorphosis and the origin of the pseudoquadrate and quadrate conditions

During most of the XIX century, the trigoniids included the single genus *Trigonia* Bruguière, but given its high diversity its numerous species were grouped into eight sections (Agassiz, 1840; Lycett, 1872–1879). The sections Clavellatae (or Clavellées) encompassed most of the species currently assigned to the genus *Myophorella*. The Quadratae (or Carrées), more quadrate in shell morphology, is comparable to the current genus *Quadratotrigonia* and some allied genera. Both sections were considered as very closely related. Steinmann (1882) added to this scheme the section Pseudoquadratae (corresponding to *Steinmanella*), regarded as a morphologic intermediate (though not a transitional form) between the Quadratae and the Clavellatae.

Even since these early studies, the similarity of the Quadratae with juveniles of the Pseudoquadratae and Clavellatae was recognized. Lycett (1872–1879) mentioned a variety (*orbignyana*) within the Quadratae species *Trigonia nodosa* J. de C. Sowerby (type species for the genus *Quadratotrigonia*) from the Cretaceous of Great Britain. According to his characterization (p. 108), the "typical" form of the species has a larger area (about half of the shell) and a more quadrate shell form. In the variety *orbignyana* the area is about 2/5 of the shell surface and the posterior margin is more oblique, resulting in a more produced and pointed posterior margin. Lycett (1872–1879: p. 8) interpreted this variety as an approximation to or a connecting link with the Clavellatae. He also mentioned that young shells of the species are shorter and more quadrate, with a larger area, and the illustrations he provided clearly show many sub-commarginal ribs in a *Freguelliella*-like pattern, as noted later on by Kobayashi and Amano (1955). Steinmann (1882) drew attention to the ontogeny of the species included in his section Pseudoquadratae, mentioning shorter juvenile shells in *T. transitoria* Steinmann, resembling the Quadratae, and becoming longer during development, like in the Clavellatae.

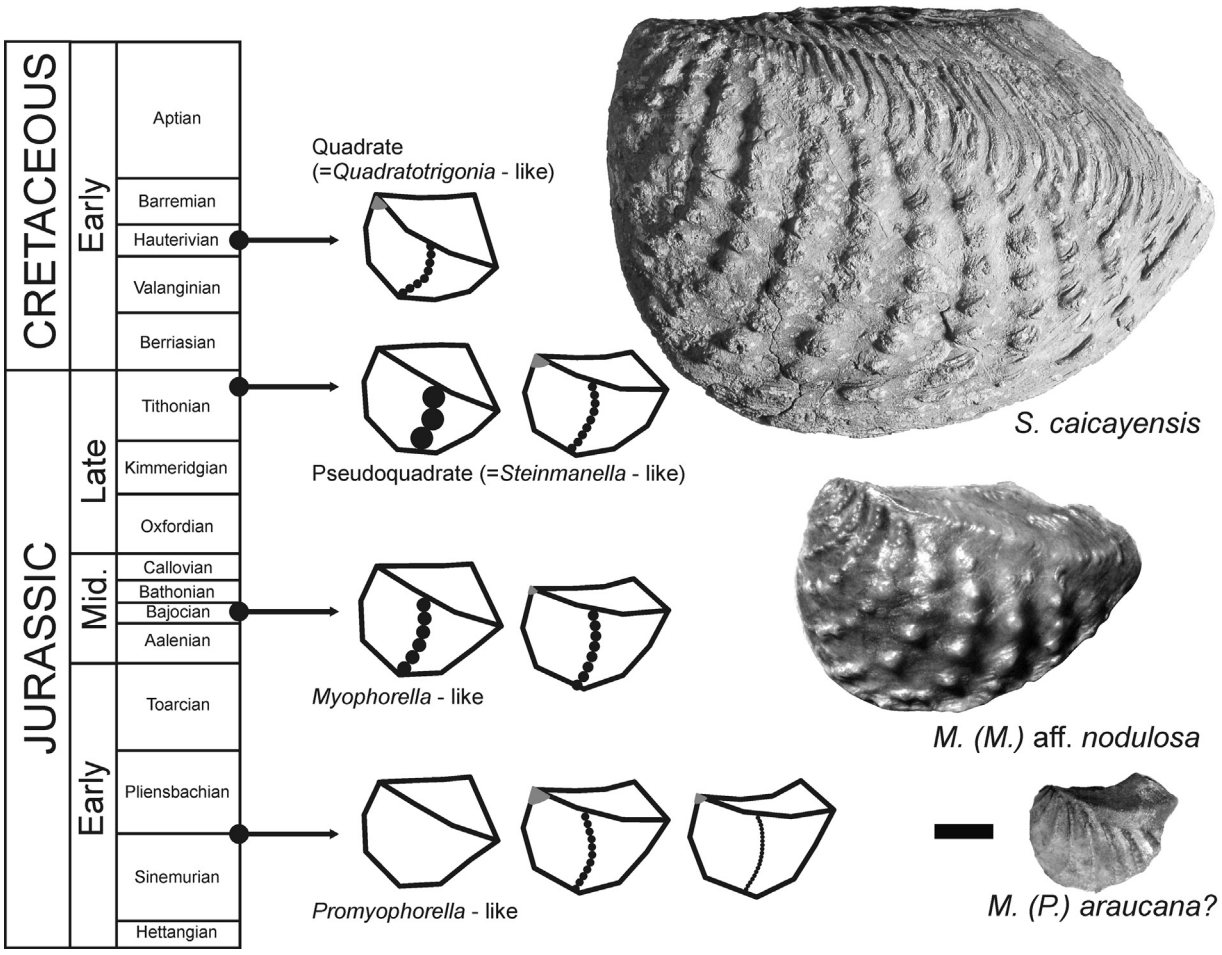

Fig. 10. Biostratigraphic scheme showing the stratigraphic appearance of each morphological type discussed in this work and their main ontogenetic stages (sketched to equal size), together with the adult size differences of the studied species (photographs). The general sketched shells represent the main ontogenetic trends for landmark and semi-landmark configurations. The *Promyophorella*-like ontogeny represents the primitive development, with a first trend of elongation and area reduction (left and middle sketches) and a second trend of opisthogyrate growth (middle and right sketches). The *Myophorella*-like and *Steinmanella*-like ontogenies reduce or even loose the second trend, while the *Quadratotrigonia*-like ontogeny most likely has only a reduced first trend. Tubercle relative size and disposition (rows of circles within the landmark configurations) seem to be paedomorphic in *Myophorella*-, *Steinmanella*- and *Quadratotrigonia*-like morphologies. Relative extent of sub-commarginal flank costae (grey triangles near the umbos) is paedomorphic in *Steinmanella*- and *Quadratotrigonia*-like morphologies. Morphological data for *Quadratotrigonia* estimated from Lycett (1872–1879). Scale bar: 10 mm (photographs).

The analysed species *S. caicayensis* shows many characters that can be considered as retention from a juvenile *Myophorella*-like species. The similarity between the shell shape development of *Steinmanella* and the first growth stage of *M. garatei* was already recognized by Echevarría et al. (2009). Unlike that of *M.* aff. *nodulosa*, the ontogeny of *S. caicayensis* develops only the first trend of shell shape change. The main difference between the ontogenetic trajectories of *M. garatei* and of *Steinmanella* is the slight dorsal curvature of the marginal carina in the first species. In *Steinmanella*, the smallest landmark configurations already show a curved marginal carina. This is probably due to their larger size compared to those of *M. garatei*. Being larger, they are also wider, affecting the projection of the carina in two dimensions and making it look more curved in lateral view. At larger sizes, both morphologies tend to converge (Fig. 5(D)).

All measured ornamentation characters in *Steinmanella* can be considered as very similar to juvenile stages of *M. araucana?* The production of strong, knob-like and spaced tubercles, as already explained for *Myophorella* s.s., can be considered as a juvenile character. The production of the different costae types (Table 4) is also strongly suggestive of retention of a juvenile feature. All myophorellids have some sub-commarginal ribs on the flank, continuous with those of the area and without tubercles in most cases; this kind of ornamentation quite resembles the ornamentation of *Frenguelliella*, the genus from which *Myophorella* is most probably derived (through *Jaworskiella* A. Leanza). Nevertheless, it must be pointed out that this kind of ornamentation is also present in other trigoniid taxa, like *Prosogyrotrigonia* Krumbeck. This kind of pattern is usually developed on the first two or three flank ribs of *Myophorella* (even in *Myophorella* s.s.; Fig. 3(A, B)). In *Steinmanella* up to five sub-commarginal costae can be found (Fig. 3(C)), and the transition with the next type of costae is more gradual. Finally, costal disposition on the marginal carina in *S. caicayensis* can also be considered as a paedomorphic pattern. The differences in slope and intercept values of *S. caicayensis* after size standardization when compared to *M. araucana?* are very similar to those obtained from the calculation of the expected paedomorph pattern (Fig. 8(B)). So the costal arrangement in *Steinmanella* actually looks like a paedomorphic retention of the costal disposition observed in *M. araucana?*, which is also scaled due to differences in size (Fig. 8(A)).

From these data, it can be confidently concluded that *Steinmanella* is a paedomorphic taxon, evolving from some *Myophorella* species and advancing further than *Myophorella* s.s.

on the paedomorphic trend (Fig. 10). The Quadratae show an even more juvenile shell morphology (Fig. 10), being relatively shorter, with a more transverse posterior margin and a larger area.

Steinmann (1882) already suggested the convergence between the Quadratae and the Pseudoquadratae. This convergence was accepted by some later authors (Kobayashi and Amano, 1955; Nakano, 1968; Levy de Caminos, 1969; Poulton, 1977; Camacho and Olivero, 1985; Cooper, 1991), while rejected by others (Cox, 1952; Saveliev, 1958). Nakano (1968), based on the V-shaped costae on the umbonal region, considered *Quadratotrigonia*, *Asiatotrigonia* Cox, *Korobkovitrigonia* Saveliev, and *Litschkovitrigonia* Saveliev as evolving from *Orthotrigonia* Cox within the Vaugoniinae, and so considered them as convergent with *Steinmanella*. The evidence provided by Nakano (1968) suggests that the pseudoquadrate and quadrate shell shape can appear repeatedly in the fossil record by some heterochronic process, like the *Myophorella* s.s. morphology. As a consequence of this, caution must be taken when trying to establish relationships based on shell morphology alone, and new non-paedomorphic characters should be tracked in order to establish the lineages within the Myophorellidae.

Based on the strong similarity in shell form and tubercle development in both genera, Kobayashi and Amano (1955) considered that *Steinmanella* evolved from some species of *Myophorella* s.s. Although it is not unlikely that *Steinmanella* evolved from a *Myophorella*-like morphology, additional characters should be looked for in order to relate it to the lineage of *Myophorella nodulosa*. Flank and anterior area ornamentations are similar in both lineages (as among most Myophorellidae), and they also share the presence of tubercles next to the submedian sulcus of the area. But they also bear some differences in ornamentation that suggest they are two different evolutionary lines. The escutcheon of the group of *M. nodulosa* is smooth, unlike many other *Myophorella* species were area costae cross the escutcheon carina and extend through the escutcheon as transverse ribs, usually with small tubercles. In *Steinmanella* the escutcheon often bears commarginal lines of tubercles, which may align in transverse rows; this can be seen in other species of the genus (Luci and Lazo, 2012: figs. 5, 6, 8, 10). The strong posterior rugae on the area of *Steinmanella* are a distinctive character of the genus, and seem also to be related to the paedomorphic morphology since large, irregular transverse plications on the posterior part of the area are also described for *Q. nodosa* (Lycett, 1872–1879: p. 107). Although the area of *M.* aff. *nodulosa* bears some growth striae posteriorly, there are other species with stronger ridges developed. So, the ancestry of the genus *Steinmanella* should not be looked for in the lineage of *M. nodulosa* but in some Jurassic *Myophorella* species (either *Promyophorella*- or *Myophorella*-like) with an ornamented escutcheon and well developed ridges on the posterior area. The earliest *Steinmanella* species in the fossil record are probably *S. vyschetzkii* (Cragin) from the Tithonian of Texas, and *S. erycina* (Philippi) and *S. haupti* (Lambert) from the Late Tithonian of west-central Argentina (H. Leanza, 1993). Given the high diversity of *Myophorella* in the Middle and Late Jurassic of North America (Poulton, 1979), the origin of *Steinmanella* should probably be tracked there.

4.4. Inferring the process and its evolutionary implications

4.4.1. Inferring the main process

Despite not knowing the precise ancestor of each paedomorph identified, they are all clearly related within the Myophorellidae. The observed adult morphological stages appear ordered in the fossil record, with the "most paedomorphic" morphology appearing later (Fig. 10). This can be considered as a large-scale paedomorphocline. According to McNamara (1982), this kind of phylogenetic trend can be the result of periodical selection of paedomorphic features.

Coupled with this paedomorphic trend, an increase in size seems also to be associated. Differences in size among the analysed species can be clearly seen on Fig. 10. Francis and Hallam (2003) found a relative increase in size during the transitions between many of the *Myophorella* species from Europe, usually coupled with some paedomorphic pattern. The species *M. (M.) dekaiboda* is also the largest *Myophorella* species in Japan and bears prominent and robust tubercles (Kobayashi and Tamura, 1955). The ancestral species for the genus *Steinmanella* is not known; nevertheless, the large size and heavy shell are characteristic features of the genus.

Gould (1977) drew attention to the evolutionary and ecological significance of heterochronic processes. Similar morphological results (in this case, paedomorphosis) can be produced by quite different processes, each one bearing different ecological and evolutionary implications. A paedomorphic pattern can be caused by hypomorphosis (earlier cessation time of the growth pattern in the descendant), deceleration (slower rate of morphologic development in the descendant), post-displacement (later onset time of the growth pattern in the descendant) or a combination of more than one of them (Alberch et al., 1979; McNamara, 1986; see Reilly et al., 1997 for a discussion on the terminology). Unfortunately, age data are essential to document these processes (McKinney, 1988, 1999), and even more, heterochronic alterations are rarely "pure", and a final pattern can result from the interaction of various processes (Klingenberg and Spence, 1993; Jones and Gould, 1999). McKinney (1988) provided a scheme to define the allometries that can be found in heterochronic analyses, considering these main heterochronic processes. The pattern found in *M.* aff. *nodulosa* and *S. caicayensis* fits as an allometric deceleration in that scheme.

Fig. 9 shows the scores for OM1, representing the first trend of shell shape development, which is the only one present in all analysed species. An allometric deceleration (i.e., lower rates of shape development relative to size) can be clearly concluded for *M.* aff. *nodulosa* and *S. caicayensis*. Also, a clear asymptote can be seen in *M. garatei* and *M. araucana?*, indicating a cessation of the development of the trait (Fig. 9). Therefore, this trend did not act during the whole life of the organism. In *M.* aff. *nodulosa* and in *S. caicayensis* an asymptote is not found, so the first trend acted during the whole life in these species, and the cessation time of the trait was the time of death. If rate of morphologic development (relative to age) was unaltered, then *M.* aff. *nodulosa* and *S. caicayensis* had far shorter life cycles than *M. araucana?* But also, considering the size differences between species, this scenario would imply astonishingly higher rates of size increase. This strongly suggests that the allometric deceleration found in *M.* aff. *nodulosa* and *S. caicayensis* was caused, most likely, by the heterochronic process of deceleration. The data for costal disposition obtained for *Steinmanella* also suggest deceleration as the responsible for the paedomorphic pattern. The lower value of slope for the standardized data (Fig. 8(B)) points to a retention of a juvenile rate of costa production rather than a sudden cessation at early stages. On the other hand, the larger intercept values on the unstandardized data (Fig. 8(A)) also suggest that the size change was achieved, at least in part, by a higher rate in size increase. It is noteworthy that, unlike in other bivalve groups (e.g., Crampton and Maxwell, 2000) size and shape seem to be independent within the Myophorellidae.

As already highlighted by Alberch and Blanco (1996), heterochrony is not a mechanism that constrains ontogenetic transformation, but a consequence of constraints in development. Under a conservative ontogeny, parallelisms and convergences would be expected from heterochrony. The recurrent evolution of the pseudoquadrate and quadrate shell shape and ornamentation

seems to be linked to the recurrent deceleration of the generalized or primitive developmental pattern of many traits within the group. The independence in the heterochronic change of the analysed characters (Fig. 10) can also help to explain other patterns found in the fossil record. Francis and Hallam (2003) found a punctuated change in the evolution of *Myophorella (P.) striata* (J. Sowerby) from *M. (P.) spinulosa*. During this transition, size increases and shell shape changes from elongate to pseudoquadrate, though maintaining the *Promyophorella*-like ornamentation on the flank. This suggests a deceleration of shell shape development without affecting ornamentation.

Nevertheless, there are also some morphological peculiarities on certain species which do not follow the general paedomorphic pattern. For example, the increased rostration in *M. irregularis* compared to its suggested ancestor (Francis and Hallam, 2003), is likely to be a peramorphic pattern. In the same way, the strong elongation in *M. incurva* suggests a peramorphic morphology from an ancestor dominated by the first trend of development of the generalized shell shape developmental pattern (*M. nodulosa* according to Francis and Hallam, 2003). In a similar way, the strong elongation in the subgenus *Steinmanella (Macrotrigonia)* Camacho and Olivero is suggestive of an extension of the ontogenetic trajectory of the genus beyond the adult morphology of other species, so it may be considered as a peramorph within the group.

4.4.2. Evolutionary/adaptive cause

Under K-selected trends deceleration can be an "'escape" from overspecialization (Gould, 1977). If the time of maturation is delayed and the life cycle is extended, deceleration of the rate of morphological change can help to avoid overdevelopment of specialized structures with dedicated functions. If this were the case, then these morphologies would arise in more stable environments, allowing individuals to reach larger sizes and longer life cycles without developing an extreme opisthogyrate morphology. Many references can be found in the literature for stable and low energy environments for *Myophorella* s.s. and the quadrate morphologies. Stanley (1977) mentioned that strongly nodose trigoniids (like *Q. nodosa* and many species of *Myophorella*) seem to be found in sediments with high percentage of mud-sized particles more frequently than species with other kind of ornamentation. According to Francis and Hallam (2003), many *Myophorella* species inhabited low energy environments dominated by fine-grained deposits. Lazo (2003) recorded *Steinmanella* shells from intermediate to high-energy shoreface and low energy offshore deposits, but he highlighted periodical colonizations of low energy muddy bottoms in the offshore during increased oxygen levels and reduced net sedimentation. Luci and Lazo (2012) interpreted the provenance environments of the lower Valanginian remains of *Steinmanella* as basinal/outer ramp to mid-ramp with storm influence; lithology is fine-grained with some rudstone beds.

An alternative, or maybe complementary hypothesis would be that some of the paedomorphic features provide advantages in the environment inhabited by the paedomorph. Stanley (1977) demonstrated that the knobs on the shell surface of *Q. nodosa* aided in burrowing in muddy substrata: cohesive sediment packs against a row of knobs, which then acts as a costa. This explanation was accepted by Francis and Hallam (2003) for the function of ornamentation of *Myophorella (Promyophorella)* on fine sand sediments. For some *Myophorella (Myophorella)* species, on the other hand, they considered the strong tubercles as futile as a burrowing aid in muddy substrates, since adduction of the valves liquifies the sediment which, in this particular case, remains liquified for a long time. Instead, they suggested that, in that case, tubercles may have aided the anchoring once burrowing ended, offering a greater surface to grip sediment. So, probably deceleration coupled with size increase acted more than once within the *Myophorella* lineage, maybe offering a quick adaptation to somewhat muddy sediments, but also allowing for longer life cycles in stable environments.

5. Conclusions

Within the subgenus *Myophorella (Promyophorella)* and its descendants, a two-trend shell shape development can be considered as primitive. The first trend is marked by a relative reduction of the posterior margin (and hence the area) together with a relative elongation of the shell. Tangent growth developed during the second growth trend, resulting in an opisthogyrate, somewhat rostrate shell. The onset time of the second growth trend occurred before the cessation of the first growth trend, so a transitional stage where both trends acted together can be identified. Flank ornamentation was characterized by two or three sub-commarginal costae, continuous through the area, after which oblique costae bearing fine tubercles started to form. Later on, costae tend to loose contact with the marginal carina due to the development of the antecarinal sulcus.

Development in *Myophorella* s.s. evolved by a paedomorphic retention of a juvenile shell shape (most likely by deceleration) coupled with a size increase, resulting in a large shell with coarse tubercles. Shell development seems to stop at the beginning of the primitive transitional stage, resulting in a slightly opisthogyrate shell.

Development in *Steinmanella* evolved by a paedomorphic suppression of the primitive second trend in the development of the shell (probably by deceleration) and most likely a size increase, resulting in a large orthogyrate shell. Ornamentation seems to be also affected by a deceleration process, resulting in the production of coarse tubercles, but also in an extended duration (relative to size) of the *Frenguelliella*-stage of costae development. Costae disposition along the carina is also affected by this retardation. The genus *Quadratotrigonia* seems to have developed even further in this paedomorphic trend, resulting in a quadratae shell shape typical of the smallest juveniles of *Steinmanella* species.

The paedomorphic (most likely decelerated) retention of juvenile shell morphology in the Myophorellidae seems to have been recurrent within the group, resulting in many cases of convergence, and obscuring the phylogenetic relationships among its species. This recurrence may be the result of different episodes of colonization of somewhat stable and low energy environments.

Acknowledgements

I thank the authorities of the Servicio Nacional de Geología y Minería (SERNAGEOMIN), Santiago, Chile, of the Museo Carmen Funes, Plaza Huincul, Argentina, and of the Museo Olsacher, Zapala, Argentina, for assistance during visits to their collections, and to the Secretary of Cultural Heritage of Neuquén Province for arranging the loans of the material collected by me. Susana Damborenea, Miguel Manceñido and Néstor Toledo are also thanked for the critical reading of previous versions of the manuscript. The useful comments of Jean-Louis Dommergues and Simon Kelly (reviewers), as well as Emmanuel Fara and Gilles Escarguel (editors) helped to largely improve this manuscript and are also highly appreciated. This work was funded by a post-doctoral scholarship from CONICET.

References

Agassiz, L., 1840. Études critiques sur les mollusques fossiles, Mémoire sur les trigonies. Petitpierre, Neuchâtel.

Alberch, P., Blanco, M.J., 1996. Evolutionary patterns in ontogenetic transformation: from laws to regularities. International Journal of Developmental Biology 40, 845–858.
Alberch, P., Gould, S.J., Oster, G.F., Wake, D.B., 1979. Size and shape in ontogeny and phylogeny. Paleobiology 5, 296–317.
Camacho, H.H., Olivero, E.B., 1985. El género Steinmanella Crickmay, 1930 (Bivalvia, Trigoniidae) en el Cretácico Inferior del Sudoeste Gondwánico. Anales de la Academia Nacional de Ciencias Exactas, Físicas y Naturales 37, 41–62.
Cooper, M.R., 1991. Lower Cretaceous Trigonioida (Mollusca, Bivalvia) from the Algoa Basin, with a revised classification of the order. Annals of the South African Museum 100, 1–52.
Cooper, M.R., 2015. On the Pterotrigoniidae (Bivalvia, Trigoniida): their biogeography, evolution, classification and relationships. Neues Jahrbuch für Geologie und Paläontologie, Abhandlung 277, 11–42.
Cox, L.R., 1952. Notes on the Trigoniidae with outlines of a classification of the family. Proceedings of the Malacological Society 29, 45–70.
Crampton, J.S., Maxwell, P.A., 2000. Size: all it's shaped up to be? Evolution of shape through the lifespan of the Cenozoic bivalve Spissatella (Crassatellidae). In: Harper, E.M., Crame, J.A., Taylor, J.D. (Eds.), The evolutionary biology of the Bivalvia. Geological Society of London Special Publication 177, 399–423.
Crickmay, C.H., 1932. Contributions toward a monograph of the Trigoniidae. American Journal of Science 24, 443–464.
Echevarría, J., 2013. Morphological trends and environment: a case study on Early Cretaceous Myophorelloidea (Bivalvia, Trigoniida) from Neuquén Basin, Argentina. Lethaia 46, 518–539.
Echevarría, J., 2014a. Ontogeny and autecology of an Early Cretaceous trigoniide species (Mollusca: Bivalvia) from Neuquén Basin, Argentina. Acta Palaeontologica Polonica 59, 407–420.
Echevarría, J., 2014b. Ontogeny of the species of *Scabrotrigonia* from the Maastrichtian Ripley Formation, USA. In: Abstract Volume, 4th International Palaeontological Congress. p. 702.
Echevarría, J., Damborenea, S.D., Manceñido, M.O., 2009. Variación ontogenética en *Myophorella* y *Steinmanella* (Trigonioida – Bivalvia) del Cretácico Inferior de Cuenca Neuquina y sus implicaciones filogenéticas. Suplemento Resúmenes, Ameghiniana 46, 73R–74R.
Fleming, C.A., 1987. New Zealand Mesozoic bivalves of the superfamily Trigoniacea. New Zealand Geological Survey Paleontological Bulletin 53, 1–104.
Francis, A.O., Hallam, A., 2003. Ecology and evolution of Jurassic trigoniid bivalves in Europe. Lethaia 36, 287–304.
Gould, S.J., 1977. Ontogeny and Phylogeny. Harvard University Press, Cambridge, Massachusetts.
Hall, T.S., 1901. Growth stages in modern trigonias, belonging to the section Pectinatae. Proceedings of the Royal Society of Victoria 14, 17–21.
Hammer, Ø., Harper, D.A.T., Ryan, P.D., 2001. PAST: Paleontological Statistics software package for education and data analysis. Palaeontologia Electronica 4, 1–9.
Jones, D.S., Gould, S.J., 1999. Direct measurement of age in fossil *Gryphaea*: the solution to a classic problem in heterochrony. Paleobiology 25, 158–187.
Kelly, S., 1995. New Trigonioid bivalves from the Early Jurassic to earliest Cretaceous of the Antarctic Peninsula region: systematics and austral paleobiogeography. Journal of Paleontology 69, 66–84.
Klingenberg, C.P., Spence, J.R., 1993. Heterochrony and allometry: lessons from the water strider genus *Limnoporus*. Evolution 47, 1834–1853.
Kobayashi, T., 1954. Studies on the Jurassic trigonians in Japan. Part 1, preliminary notes. Japanese Journal of Geology and Geography 25, 61–80.
Kobayashi, T., Amano, M., 1955. On the Pseudoquadratae Trigonians, *Steinmanella*, in the Indo-Pacific Province. Japanese Journal of Geology and Geography 26, 193–208.
Kobayashi, T., Mori, K., 1955. The Vaugoniinae from the Kitakami Mountains in North Japan. On the Jurassic Trigonians in Japan, part III. Japanese Journal of Geology and Geography 26, 73–88.
Kobayashi, T., Tamura, M., 1955. The Myophorellinae from North Japan, Studies on the Jurassic Trigonians in Japan, part IV. Japanese Journal of Geology and Geography 26, 89–103.
Lazo, D.G., 2003. The genus *Steinmanella* (Bivalvia, Trigonioida) in the Lower Member of the Agrio Formation (Lower Cretaceous), Neuquén Basin, Argentina. Journal of Paleontology 77, 1069–1085.
Leanza, A.F., 1942. Los Pelecípodos del Lias de Piedra Pintada en el Neuquén. Revista del Museo de La Plata (Nueva Serie) sección paleontología 2, 143–206.
Leanza, H.A., 1993. Jurassic and Cretaceous trigoniid bivalves from West-Central Argentina. Bulletins of American Paleontology 105, 1–95.
Leanza, H.A., Garate-Zubillaga, J.I., 1987. Faunas de trigonias (Bivalvia) del Jurásico y Cretácico inferior de la Provincia del Neuquén, Argentina, conservadas en el Museo Juan Olsacher de Zapala. In: Volkheimer, W. (Ed.), Bioestratigrafía de los Sistemas Regionales del Jurásico y Cretácico de América del Sur. Comité Sudamericano del Jurásico y Cretácico, Mendoza, pp. 201–255.
Levy, R., 1966. Revisión de las trigonias de Argentina. I. – Una nueva especie de *Myophorella* del Lías de la Pampa de Agnia (Chubut), con consideraciones acerca de la presencia de Myophorellinae en Argentina. Ameghiniana 4, 237–241.
Levy de Caminos, R., 1969. Revisión de las trigonias de la Argentina. Parte V: El grupo de las Pseudoquadratae. Ameghiniana 6, 65–68.
Luci, L., Lazo, D.G., 2012. The genus *Steinmanella* Crickmay (Bivalvia) in the transition between the Vaca Muerta and Mulichinco formations, early Valanginian, Neuquén Basin, Argentina. Ameghiniana 49, 96–117.
Lycett, J., 1872–1879. A monograph of the British fossil Trigoniae. Monographs of the Palaeontographical Society, London 26, 1–245 (28, 29, 31, 33).
Maeda, S., Kawabe, T., 1966. Note on the ontogenetic change of *Myophorella (Promyophorella) orientalis*. Annual Report of the Foreign Students' College of Chiba University 1, 51–56.
March, M.C., 1911. Studies in the morphogenesis of certain Pelecypoda. (3) The ornament of *Trigonia clavellata* and some of its derivatives. Memoirs and Proceedings of the Manchester Literary and Philosphical Society 55 (2), 1–13 (reprint pagination).
McKinney, M.L., 1988. Classifying heterochrony: allometry, size and time. In: McKinney, M.L. (Ed.), Heterochrony in Evolution: A Multidisciplinary Approach. Plenum Press, New York, pp. 17–34.
McKinney, M.L., 1999. Heterochrony: beyond words. Paleobiology 25, 149–153.
McKinney, M.L., McNamara, K.J., 1991. Heterochrony: the evolution of ontogeny. Plenum Press, New York.
McNamara, K.J., 1982. Heterochrony and phylogenetic trends. Paleobiology 8, 130–142.
McNamara, K.J., 1986. A guide to the nomenclature of heterochrony. Journal of Paleontology 60, 4–13.
Nakano, M., 1968. On the Quadratotrigoniinae. Japanese Journal of Geology and Geography 39, 27–41.
Pérez, E., Aberhan, M., Reyes, R., von Hillebrandt, A., 2008. Early Jurassic Bivalvia of northern Chile. Part III. Order Trigonioida. Beringeria 39, 51–102.
Pérez, E., Reyes, R., 1977. Las trigonias Jurásicas de Chile y su valor cronoestratigráfico. Instituto de Investigaciones Geológicas – Chile, Boletín 30, 1–58.
Poulton, T.P., 1977. Early Cretaceous trigoniid Bivalves of Manning Provincial Park, southwestern British Columbia. Geological Survey of Canada Paper 76–9, 1–25.
Poulton, T.P., 1979. Jurassic trigoniid bivalves from Canada and western United States of America. Geological Survey of Canada, Bulletin 282, 1–82.
Reilly, S.M., Wiley, E.O., Meinhardt, D.J., 1997. An integrative approach to heterochrony: the distinction between interspecific and intraspecific phenomena. Biological Journal of the Linnean Society 60, 119–143.
Rohlf, F.J., 2008. tpsDig2. (Available at: http://life.bio.sunysb.edu/morph/).
Rudra, P., Bardhan, S., 2006. Status of "*Trigonia ventricosa*" (Bivalvia) from the Upper Jurassic-Lower Cretaceous of Kutch, western India: Kitchin's unfinished synthesis. Cretaceous Research 27, 611–628.
Sato, T., Taketani, Y., 2008. Late Jurassic to Early Cretaceous ammonite fauna from the Somanakamura Group in northeast Japan. Paleontological Research 12, 261–282.
Saveliev, A.A., 1958. Nizhnemelovye trigoniidy Mangyshlaka i zapadnoï Turkmenii (s ocherkom sistematiki i filogenii cemeistva). Trudy Vsesoyuznogo Neftyanogo Nauchno-issledovateskogo Geologorazvedochnogo Instituta (VNIGRI) 125, 1–386 (In Russian).
Schneider, S., Kelly, S.R.A., 2014. A global perspective of the Trigoniida (Bivalvia: Palaeoheterodonta), with a focus on their Mesozoic and Cenozoic representatives. In: Abstract Volume, 4th International Palaeontological Congress. p. 610.
Sheets, H.D., 2001. IMP: Integrated Morphometrics Package. Department of Physics, Canisius College, Buffalo, NY (Available at: http://www3.canisius.edu/~sheets/morphsoft.html – http://www3.canisius.edu/~sheets/moremorph.html).
Sheets, H.D., 2003. IMP: Integrated Morphometrics Package. Department of Physics, Canisius College, Buffalo, NY (Available at: http://www3.canisius.edu/~sheets/morphsoft.html – http://www3.canisius.edu/~sheets/moremorph.html).
Stanley, S.M., 1977. Coadaptation in the Trigoniidae, a remarkable family of burrowing bivalves. Palaeontology 20, 116–119.
Steinmann, G., 1882. Die Gruppe der Trigoniae pseudoquadratae. Neues Jahrbuch für Mineralogie, Geologie und Paläontologie 1, 219–228.
Zelditch, M.L., Swiderski, D.L., Sheets, H.D., Fink, W.L., 2004. Geometric Morphometrics for Biologists: a Primer. Elsevier Academic Press, Amsterdam.